with this is the observation of two distinct forms of resistin—the HMW hexamer and the LMW form—in serum and adipocyte-conditioned medium. The LMW form displays significantly increased bioactivity. The overall multimeric assembly of the resistin family is similar to that of adiponectin. The comparable domain architecture of these two adipocyte-specific hormones, despite diametrically opposed physiological effects, suggests a common regulatory mechanism and points to new avenues of research focusing on modulation of adipokine secretion and activity by cysteine-mediated complex formation or processing.

References and Notes

1. C. L. Ogden, K. M. Flegal, M. D. Carroll, C. L. Johnson, *JAMA* **288**, 1728 (2002).
2. K. M. Flegal, M. D. Carroll, C. L. Ogden, C. L. Johnson, *JAMA* **288**, 1723 (2002).
3. J. J. Reilly *et al*., *Arch. Dis. Child.* **88**, 748 (2003).
4. U. S. Census, *Bureau of the Census, 2000 Census Estimates;* www.cdc.gov/diabetes/pubs/estimates.htm.
5. I. M. Jazet, H. Pijl, A. E. Meinders, *Neth. J. Med.* **61**, 194 (2003).
6. T. Fujita *et al*., *Diabetes* **32**, 804 (1983).
7. T. Fujiwara, S. Yoshioka, T. Yoshioka, I. Ushiyama, H. Horikoshi, *Diabetes* **37**, 1549 (1988).
8. P. E. Beales, P. Pozzilli, *Diabetes Metab. Res. Rev.* **18**, 114 (2002).
9. H. Hauner, *Diabetes Metab. Res. Rev.* **18** (suppl. 2), S10 (2002).
10. R. R. Henry, *Endocrinol. Metab. Clin. North Am.* **26**, 553 (1997).
11. M. W. Rajala, P. E. Scherer, *Endocrinology* **144**, 3765 (2003).
12. A. H. Berg, T. P. Combs, X. Du, M. Brownlee, P. E. Scherer, *Nature Med.* **7**, 947 (2001).
13. C. M. Steppan *et al*., *Nature* **409**, 307 (2001).
14. T. P. Combs *et al*., *Endocrinology* **143**, 998 (2002).
15. I. N. Holcomb *et al*., *EMBO J.* **19**, 4046 (2000).
16. K. H. Kim, K. Lee, Y. S. Moon, H. S. Sul, *J. Biol. Chem.* **276**, 11252 (2001).
17. M. W. Rajala *et al*., *Mol. Endocrinol.* **16**, 1920 (2002).
18. C. M. Steppan *et al*., *Proc. Natl. Acad. Sci. U.S.A.* **98**, 502 (2001).
19. B. Gerstmayer *et al*., *Genomics* **81**, 588 (2003).
20. M. W. Rajala, S. Obici, P. E. Scherer, L. Rossetti, *J. Clin. Invest.* **111**, 225 (2003).
21. R. R. Banerjee *et al*., *Science* **303**, 1195 (2004).
22. T. P. Combs, A. H. Berg, S. Obici, P. E. Scherer, L. Rossetti, *J. Clin. Invest.* **108**, 1875 (2001).
23. P. E. Scherer, S. Williams, M. Fogliano, G. Baldini, H. F. Lodish, *J. Biol. Chem.* **270**, 26746 (1995).
24. L. Shapiro, P. E. Scherer, *Curr. Biol.* **8**, 335 (1998).
25. U. B. Pajvani *et al*., *J. Biol. Chem.* **278**, 9073 (2003).
26. U. B. Pajvani *et al*., *J. Biol. Chem.* **279**, 12152 (2004).
27. Materials and methods are available as supporting material on *Science* Online.
28. Z. Dauter, M. Dauter, K. R. Rajashankar, *Acta Crystallogr. D Biol. Crystallogr.* **56**, 232 (2000).
29. L. Holm, C. Sander, *Nucleic Acids Res.* **26**, 316 (1998).
30. R. R. Banerjee, M. A. Lazar, *J. Biol. Chem.* **276**, 25970 (2001).
31. D. L. Brasaemle *et al*., *J. Lipid Res.* **38**, 2249 (1997).
32. T. Anelli *et al*., *EMBO J.* **22**, 5015 (2003).
33. W. L. DeLano (2002), http://pymol.sourceforge.net
34. H. Nielsen, J. Engelbrecht, S. Brunak, G. von Heijne, *Protein Eng.* **10**, 1 (1997).

35. We thank the personnel of Advanced Photon Source (APS) beamlines 31-ID and 32-ID; National Synchrotron Light Source beamlines X4, X9, and X25; and A. Gogos and T. Boggon for help with data collection; M. Collins, A. Gogos, and D. Brasaemle for help with biochemical experiments; and F. P. Davis and A. Sali for help with solvent accessibility calculations. We also thank Z. Wang, J.-Y. Kim, and A. Narwocki for help at various stages of this project. We are grateful to W. A. Hendrickson and P. D. Kwong for critical comments. The structures reported in this paper have been deposited in the PDB as 1RFX, 1RGX, and 1RH7. This work was supported in part by grants from NIH and the Research to Prevent Blindness Foundation. Part of this work was performed as part of the National Institute of General Medical Sciences' New York Structural Genomics Research Consortium (NYSGXRC). Use of the APS was supported by the U.S. Department of Energy, Office of Science, Office of Basic Energy Science, under Contract No. W-31-109-Eng-38. Use of the SGX Collaborative Access Team (SGX-CAT) beamline facilities at sector 31 of the APS was provided by Structural GenomiX, Inc., which constructed and operates the facility.

Supporting Online Material

www.sciencemag.org/cgi/content/full/304/5674/1154/DC1
Materials and Methods
Figs. S1 to S3
Table S1
References

10 November 2003; accepted 19 April 2004

Hereditary Early-Onset Parkinson's Disease Caused by Mutations in *PINK1*

Enza Maria Valente,[1]*‡ Patrick M. Abou-Sleiman,[2]* Viviana Caputo,[1,3]† Miratul M. K. Muqit,[2,4]† Kirsten Harvey,[5] Suzana Gispert,[6] Zeeshan Ali,[6] Domenico Del Turco,[7] Anna Rita Bentivoglio,[9] Daniel G Healy,[2] Alberto Albanese,[10] Robert Nussbaum,[11] Rafael González-Maldonado,[12] Thomas Deller,[7] Sergio Salvi,[1] Pietro Cortelli,[13] William P. Gilks,[2] David S. Latchman,[4,14] Robert J. Harvey,[5] Bruno Dallapiccola,[1,3] Georg Auburger,[8]‡ Nicholas W. Wood[2]‡

Parkinson's disease (PD) is a neurodegenerative disorder characterized by degeneration of dopaminergic neurons in the substantia nigra. We previously mapped a locus for a rare familial form of PD to chromosome 1p36 (PARK6). Here we show that mutations in *PINK1* (PTEN-induced kinase 1) are associated with PARK6. We have identified two homozygous mutations affecting the PINK1 kinase domain in three consanguineous PARK6 families: a truncating nonsense mutation and a missense mutation at a highly conserved amino acid. Cell culture studies suggest that PINK1 is mitochondrially located and may exert a protective effect on the cell that is abrogated by the mutations, resulting in increased susceptibility to cellular stress. These data provide a direct molecular link between mitochondria and the pathogenesis of PD.

Parkinson's disease (PD) is a common neurodegenerative disorder that is characterized by the loss of dopaminergic neurons in the substantia nigra and the presence of cytoplasmic protein inclusions known as Lewy bodies. The majority of PD cases are sporadic; however, the identification of a number of genes responsible for rare familial forms of PD has provided important insights into the underlying mechanisms of the disease. These genes, encoding α-synuclein, parkin, UCH-L1, and DJ-1, have implicated protein misfolding, impairment of the ubiquitin-proteasome system, and oxidative stress in the pathogenesis of the disease (*1*, *2*).

We previously mapped PARK6, a locus linked to autosomal recessive, early-onset PD, to a 12.5-centimorgan (cM) region on chromosome 1p35-p36 by autozygosity mapping in a large consanguineous family from Sicily (*3*). Subsequent identification of two additional consanguineous families [one from central Italy (family IT-GR) (*4*) and one from Spain] provided additional evidence of linkage to PARK6. A critical recombination event in the Spanish family refined the candidate region to a 3.7-cM interval between flanking markers D1S2647 and D1S1539. Fine mapping of single-nucleotide polymorphisms and newly generated short tandem repeat markers in the three families defined a 2.8-megabase region of homozygosity within contig NT_004610, containing approximately 40 genes.

Candidate genes were prioritized on the basis of their putative function and expression in the central nervous system, as assessed by bioinformatic analysis and by exon amplification from a human substantia nigra cDNA library. Sequence analysis of candidate genes in affected members from each family led to the identification of two homozygous mutations in the *PTEN- induced putative kinase 1* (*PINK1*) gene. The mutations segregated with the disease phenotype in the three consanguineous families, were confirmed in the cDNA, and were absent from 400 control chromosomes, including 200 chromosomes from Sicilian individuals. The Spanish family carried a G→A

transition in exon 4 [nucleotide (nt) 11185 in NT_004610], resulting in an amino acid substitution (G309D) (*5*) at a highly conserved position in the putative kinase domain (fig. S1). Both Italian families carried the same G→A transitions in exon 7 (nt 15600 in NT_004610), which results in a W437OPA substitution, truncating the last 145 amino acids encoding the C terminus of the kinase domain. These families shared a common haplotype, implying common ancestry (table S1).

The *PINK1* gene contains eight exons spanning ~1.8 kilobases and encodes a 581–amino acid protein. The transcript is ubiquitously expressed (*6*) and is predicted to encode a 34–amino acid mitochondrial targeting motif (the cleavage site for the mitochondrial processing peptidase between residues 34 and 35) and a highly conserved protein kinase domain (residues 156 to 509) that shows high degree of homology to the serine/threonine kinases of the Ca^{2+}/calmodulin family.

To investigate the consequences of the missense mutation at the cellular level, we transiently transfected wild-type or G309D c-Myc–tagged *PINK1* cDNA constructs into monkey kidney COS-7 cells. The mutation did not alter production of mature full-length protein, which suggests that it does not significantly affect protein stability (fig. S2). Both wild-type and mutant PINK1 localized to mitochondria, as assessed by immunofluoresence microscopy of transfected COS-7 cells (Fig. 1) and human neuroblastoma SH-SY5Y cells (fig. S3). Furthermore, the mitochondrial localization of PINK1 was confirmed by Western blotting of mitochondrial enriched fractions obtained from COS-7 cells transiently transfected with c-Myc–tagged wild-type *PINK1* cDNA (Fig. 2).

We next investigated the effect of *PINK1* mutations on mitochondrial function using a fluorescence-activated cell sorting (FACS)–based assay of mitochondrial membrane potential ($\Delta\psi m$) by examining the distribution of tetramethylrhodamine methyl ester (TMRM), a fluorescent lipophilic cation. Mitochondrial membrane potential is central to mitochondrial biology: It defines the transport of ions, including Ca^{2+} uptake, and provides the driving force for oxidative phosphorylation (*7*). SH-SY5Y cells were transiently

[1]CSS IRCCS, Mendel Institute, viale Regina Margherita 261, 00198 Rome, Italy. [2]Department of Molecular Neuroscience, Institute of Neurology, Queen Square, London, WC1N 3BG, UK. [3]Department of Experimental Medicine and Pathology, University La Sapienza, Viale Regina Elena 324, 00187 Rome, Italy. [4]Medical Molecular Biology Unit, Institute of Child Health, 30 Guilford Street, London WC1N 1EH, UK. [5]Department of Pharmacology, The School of Pharmacy, 29/39 Brunswick Square, London WC1N 1AX, UK. [6]Institute for Experimental Neurobiology; [7]Institute of Clinical Neuroanatomy; [8]Section of Molecular Neurogenetics, Clinic for Neurology; J.W. Goethe University, Theodor Stern Kai 7, 60590 Frankfurt/M, Germany. [9]Institute of Neurology, Catholic University, largo A. Gemelli 8, I-00168 Rome, Italy. [10]National Neurologic Institute Carlo Besta, via Celoria 11, 20133 Milan, Italy. [11]National Human Genetics Research Institute, National Institutes of Health, 49 Convent Drive, Bethesda, MD 20892, USA. [12]Department of Neurology, Hospital Universitatio San Cecilio, Avenida Dr. Olóriz s/n, 18012 Granada, Spain. [13]Department of Neurosciences, University of Modena and Reggio Emilia, via del Pozzo 71, 41100 Modena, Italy. [14]Birkbeck, University of London, Malet Street, London WC1E 7HX, UK.

*These authors contributed equally to this work.
†These authors share joint second authorship.
‡To whom correspondence should be addressed. E-mail: n.wood@ion.ucl.ac.uk (N.W.W.); auburger@em.uni-frankfurt.de (G.A.); e.valente@css-mendel.it (E.M.V.)

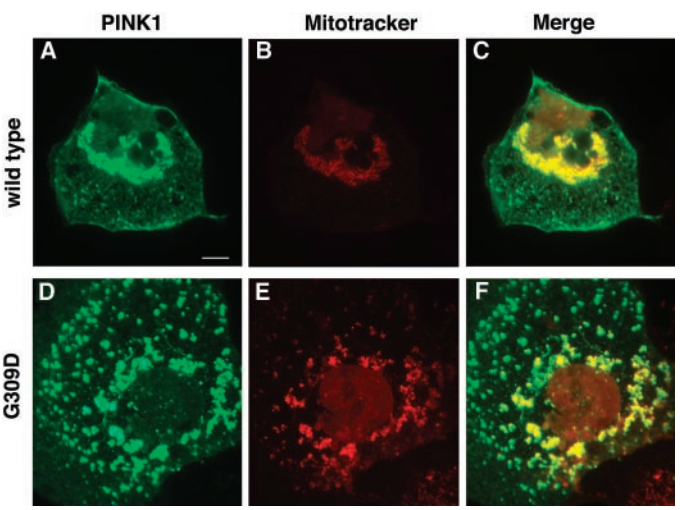

Fig. 1. PINK1 is localized to the mitochondria in mammalian cells, and its localization is not affected by the G309D mutation. COS-7 cells transfected with wild-type (**A** to **C**) or G309D (**D** to **F**) c-Myc–tagged PINK1 protein are shown. Immunofluorescence was carried out with c-Myc antibody and mitotracker as follows: c-Myc–*PINK1* [green, (A) and (D)]; mitotracker [red, (B) and (E)]; and c-Myc–*PINK1* and mitotracker merged [(C) and (F)]. Scale bar, 8.0 μm.

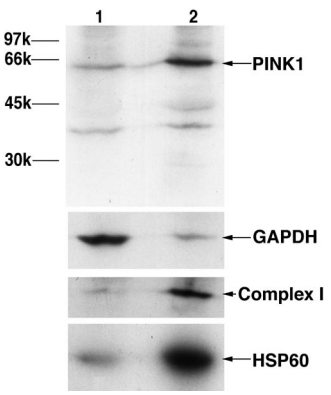

Fig. 2. PINK1 is localized to the mitochondria-enriched fraction of mammalian cells. COS-7 cells were transiently transfected with c-Myc–tagged wild-type *PINK1*. Cytoplasmic (lane 1) and mitochondria-enriched (lane 2) fractions were obtained and probed for c-Myc PINK1 expression by Western blot analysis using an antibody to c-Myc. The same membrane was stripped and reprobed with antibodies to heat shock protein 60 (HSP60), complex I, and glyceraldehyde-3-phosphate dehydrogenase (GAPDH) to determine the relative purity of fractions analyzed.

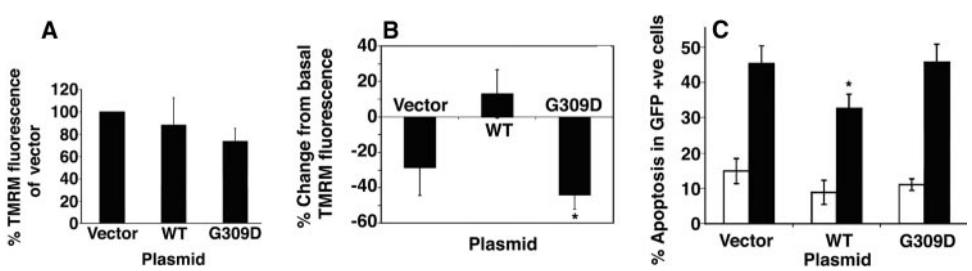

Fig. 3. Wild-type PINK1 but not mutant G309D PINK1 protects against stress-induced mitochondrial dysfunction and apoptosis. (**A** and **B**) Effect of wild-type and mutant PINK1 on mitochondrial membrane potential ($\Delta\psi m$) determined by FACS of GFP-gated events of SH-SY5Y cells treated with vehicle (basal value) or MG-132. (A) Basal TMRM values normalized to vector, mean ± SEM percent TMRM fluorescence of vector. (B) Mean ± SEM percent change in median TMRM fluorescence from the basal value for each construct after treatment with 15 μM MG-132. *P >0.01 for G309D versus wild-type PINK1; ANOVA with post-hoc Bonferroni correction; n = 8 data sets from three independent experiments performed in duplicate or triplicate. (**C**) Effect of wild-type and mutant PINK1 on apoptosis, as determined by FACS of annexin V-PE–positive GFP-gated events of SH-SY5Y cells treated with dimethyl sulfoxide vehicle (open bars) or MG-132 (solid bars). The mean ± SEM percent apoptotic cell death for each construct after treatment with vehicle or 15 μM MG-132 is shown. *P < 0.05; ANOVA, n = 12 data sets from four independent experiments performed in triplicate.

cotransfected with wild-type and mutant *PINK1* cDNA and a green fluorescent protein (GFP) reporter plasmid and then stressed with the peptide aldehyde Cbz-leu-leu-leucinal (MG-132), which inhibits the proteasome and induces apoptosis via distinct mechanisms, including mitochondrial injury (*8*). Analysis of TMRM fluorescence in GFP-positive cells revealed that the *PINK1* mutation had no significant effect on $\Delta\psi m$ under basal conditions (Fig. 3A). However, after stress with MG-132, there was a significant decrease in $\Delta\psi m$ from basal levels in cells transfected with G309D *PINK1* as compared with wild-type *PINK1* (G309D, $-44.1\% \pm 8.1$; versus wild-type *PINK1*, $13.0\% \pm 13.7$; $P < 0.01$; $n = 8$ data sets) (Fig. 3B and fig. S4).

We next studied apoptosis of MG-132–stressed SH-SY5Y cells transfected with either wild-type or G309D *PINK1* by FACS using annexin V conjugated to the fluorochrome phycoerythrin (annexin V-PE). Annexin V has a high binding affinity for the membrane phospholipid, phosphatidylserine, that is exposed on the surface of apoptotic cells. Consistent with the changes in $\Delta\psi m$ after stress, overexpression of wild-type *PINK1* but not mutant *PINK1* significantly reduced the level of apoptotic cell death induced by MG-132 in GFP-positive cells [vector, $45.4\% \pm 5.0$; wild-type *PINK1*, $32.7\% \pm 4.0$; G309D, $45.8\% \pm 5.0$; $P > 0.05$; analysis of variance (ANOVA), $n = 12$ data sets] (Fig. 3C and fig. S5). These preliminary findings suggest that wild type *PINK1* may protect neurons from stress-induced mitochondrial dysfunction and stress-induced apoptosis and that this effect is abrogated by the G309D mutation.

Several lines of evidence suggest that impairment of mitochondrial activity could represent an early critical event in the pathogenesis of sporadic PD (*2*). Environmental toxins such as 1-methyl-4-phenyl-1,2,3,6-tetrahydro-pyridin and the pesticide rotenone induce selective death of dopaminergic neurons through inhibition of complex I activity (*9*, *10*). Complex I deficiency and a variety of markers of oxidative stress have been demonstrated in postmortem brains of PD patients (*2*, *11*, *12*). In addition, several reports have shown that mitochondrial dysfunction associated with oxidative stress can trigger α-synuclein aggregation and accumulation, although the exact mechanisms remain unclear (*13*).

The *PINK1* mutations described here occur in the putative serine/threonine kinase domain and thus conceivably could affect kinase activity or substrate recognition. Altered phosphorylation has been reported as a pathogenetic mechanism in other neurodegenerative diseases, including Alzheimer's disease, tauopathy, and spinocerebellar ataxia (*14*, *15*). The recent demonstration that phosphorylation of α-synuclein at serine 129 occurs in Lewy bodies in a variety of brains from humans with synucleinopathy (*16*) suggests that altered phosphorylation may also play a role in PD. We hypothesize that PINK1 may phosphorylate mitochondrial proteins in response to cellular stress, protecting against mitochondrial dysfunction. PINK1 was originally shown to be upregulated by the tumor suppressor gene *PTEN* in cancer cells (*6*). In neurons, the PTEN signaling pathway is involved in cell cycle regulation and cell migration and promotes excitotoxin-induced apoptosis in the hippocampus (*17*). However, PINK1 has not been shown to have any effects on PTEN-dependent cell phenotypes (*6*), and its role in the PTEN pathway therefore requires further investigation.

References and Notes

1. W. Dauer, S. Przedborski, *Neuron* **39**, 889 (2003).
2. T. M. Dawson, V. L. Dawson, *Science* **302**, 819 (2003).
3. E. M. Valente *et al*., *Am. J. Hum. Genet.* **68**, 895 (2001).
4. E. M. Valente *et al*., *Ann. Neurol.* **51**, 14 (2002).
5. Single-letter abbreviations for the amino acid residues are as follows: A, Ala; D, Asp; G, Gly; W, Trp.
6. M. Unoki, Y. Nakamura, *Oncogene* **20**, 4457 (2001).
7. M. R. Duchen, A. Surin, J. Jacobson, *Methods Enzymol.* **361**, 353 (2003).
8. J. H. Qiu *et al*., *J. Neurosci.* **20**, 259 (2000).
9. W. J. Nicklas, I. Vyas, R. E. Heikkila, *Life Sci.* **36**, 2503 (1985).
10. R. Betarbet *et al*., *Nature Neurosci.* **3**, 1301 (2000).
11. A. H. Schapira *et al*., *Lancet* **2**, 1269 (1989).
12. P. Jenner, C. W. Olanow, *Ann. Neurol.* **44**, S72 (1998).
13. T. B. Sherer *et al*., *J. Neurosci.* **22**, 7006 (2002).
14. L. Buee, T. Bussiere, V. Buee-Scherrer, A. Delacourte, P. R. Hof, *Brain Res. Rev.* **33**, 95 (2000).
15. HK. Chen *et al., Cell* **113,** 457 (2003).
16. H. Fujiwara *et al*., *Nature Cell Biol.* **4**, 160 (2002).
17. D. S. Gary, M. P. Mattson, *Neuromol. Med.* **2**, 261 (2002).

18. We thank the patients and families who participated in this study, J. Sinclair for technical assistance with FACS experiments, G. Howell for bioinformatic support, M. Duchen for useful discussion, S. Eaton for assistance with mitochondrial fractionation, and Y. Nakamura and M. Unoki for the *PINK1* plasmid. Supported by grants from Telethon, Italy (E.M.V.); the Italian Ministry of Health (E.M.V. and B.D.); MURST (B.D.); the Parkinson's Disease Society, UK (N.W.W., D.S.L., R.J.H., and D.G.H.); the Brain Research Trust (P.M.A.S. and N.W.W.); and the Deutsche Forschungsgemeinschaft (G.A. and S.G.). M.M.K.M. is a Medical Research Council Clinical Research Training Fellow. GenBank accession numbers are as follows: *PINK1* genomic sequence, AL391357; PINK1 mRNAs, AB053323, AF316873, AK075225, BC009534, and BC028215; and PINK1 protein, BAB55647, AAK28062, BAC11484, AAH09534, and AAH28215.

Supporting Online Material

www.sciencemag.org/cgi/content/full/1096284/DC1
Materials and Methods
SOM Text
Figs. S1 to S5
Tables S1 and S2
References

2 February 2004; accepted 1 April 2004
Published online 15 April 2004;
10.1126/science.1096284
Include this information when citing this paper.

Genetic Structure of the Purebred Domestic Dog

Heidi G. Parker,[1,2,3] Lisa V. Kim,[1,2,4] Nathan B. Sutter,[1,2] Scott Carlson,[1] Travis D. Lorentzen,[1,2] Tiffany B. Malek,[1,3] Gary S. Johnson,[5] Hawkins B. DeFrance,[1,2] Elaine A. Ostrander,[1,2,3,4]* Leonid Kruglyak[1,3,4,6]

We used molecular markers to study genetic relationships in a diverse collection of 85 domestic dog breeds. Differences among breeds accounted for ~30% of genetic variation. Microsatellite genotypes were used to correctly assign 99% of individual dogs to breeds. Phylogenetic analysis separated several breeds with ancient origins from the remaining breeds with modern European origins. We identified four genetic clusters, which predominantly contained breeds with similar geographic origin, morphology, or role in human activities. These results provide a genetic classification of dog breeds and will aid studies of the genetics of phenotypic breed differences.

The domestic dog is a genetic enterprise unique in human history. No other mammal has enjoyed such a close association with humans over so many centuries, nor been so substantially shaped as a result. A variety of dog morphologies have existed for millennia, and reproductive isolation between them was formalized with the advent of breed clubs and breed standards in the mid–19th century. Since that time, the promulgation of the "breed barrier" rule—no dog may become a registered member of a breed unless both its dam and sire are registered members—has ensured a relatively closed genetic pool among dogs of each breed. At present, there are more than 400 described breeds, 152 of which are recognized by the American Kennel Club (AKC) in the United States (*1*). Over 350 inherited disorders have been described in the purebred dog population (*2*). Many of these mimic common human disorders and are restricted to particular breeds or groups of breeds as a result of aggressive in-